Coherence Estimation for Repeat-Pass Interferometry

Jeremy Dillon
Kraken Sonar Systems Inc.
St. John's, NL, Canada
Email: jdillon@krakensonar.com

Vincent Myers
Defence R&D Canada – Atlantic
Dartmouth, NS, Canada
Email: vincent.myers@drdc-rddc.gc.ca

***Abstract*—Repeat-pass interferometry is an extension of Synthetic Aperture Sonar (SAS) that exploits the temporal characteristics of seafloor reverberation by coherently combining echoes from multiple passes of the sonar platform. In order to achieve pass-to-pass coherence, the spatial separation between passes must be less than a value known as the critical baseline, which depends on the sonar parameters and the range-dependent imaging geometry. The temporal separation between passes must also be less than the coherence time of the seabed, which is highly environmentally dependent and which defines the maximum time interval between passes. It is also necessary to coregister the complex seabed images to within a fraction of a pixel (usually on the order of several millimeters for the centimeter resolution SAS used in mine countermeasures). This imposes strict requirements on the navigation accuracy of the sonar platform that cannot be met using inertial or underwater positioning sensors alone. This paper presents a data-driven method for estimating the repeat-pass coherence map using local coregistration of the complex SAS images from each pass. The method can be applied to any SAS without requiring access to raw acoustic data or post-processing of data from a high grade inertial navigation system. Experimental results are presented for a repeat-pass survey using AquaPix, a wideband 300 kHz interferometric SAS, installed on an ISE Arctic Explorer AUV during recent sea trials with Defence Research and Development Canada.**

I. Introduction

Coherently combining two or more Synthetic Aperture Sonar (SAS) images acquired at different times has two principal applications: Coherent Change Detection (CCD) [1] and high resolution bathymetry [2]. CCD is a promising technology for detecting changes when there is negligible variation in the mean backscattered energy by exploiting the phase of the sonar images; such changes could be caused by a new object present on the seafloor, by subtle changes in topography, or by a perturbation of the spatial distribution of the scatterers in a resolution cell. CCD can be used when the nature of the change is not known in advance, or as a data reduction or false alarm mitigation step by focusing attention on pixels in the sonar image where changes are likely to have occurred, particularly in areas of high clutter. Similarly, highly precise bathymetric maps can be produced by processing images obtained from repeated passes at different altitudes, creating a baseline that can be used to determine the topography of the seafloor. In order to apply repeat-pass techniques, pairs of images must be processed interferometrically, which places very stringent requirements on the acquisition geometry, navigational accuracy and stability of the environment. One must also coregister sonar images with sub-pixel accuracy. A corollary application of the coregistration step is the ability to produce a very accurate position correction for Autonomous Underwater Vehicles (AUVs) to help overcome the unavoidable drift of inertial navigation systems, allowing long missions to be performed without having to breach the surface for a position update. This is useful in operations under ice, in areas with high surface traffic, or when covertness is desired.

This paper presents a data-driven method for estimating the repeat-pass coherence map using local coregistration of the complex SAS images from each pass. The method can be applied to any SAS without requiring access to raw acoustic data or post-processing of data from a high grade inertial navigation system (unlike other techniques that require images to be iteratively re-focused as the navigation solution is refined [3]). Additionally, the method is sufficiently simple to implement that it raises the interesting possibility of performing CCD in near real-time onboard an AUV as part of an adaptive concept of operations for target detection and classification. Experimental results are presented for a repeat-pass survey using AquaPix, a wideband 300 kHz interferometric SAS, installed on an ISE Arctic Explorer AUV during recent sea trials with Defence Research and Development Canada (DRDC). The coherence between SAS images was computed at 25×25 cm resolution. Coregistration was performed locally using a wideband cross-correlation followed by truncated sinc interpolation. It is shown that local coregistration improves the coherence without requiring any refocusing of the synthetic aperture images. This technique is therefore ideal for CCD where it is necessary to minimize the decoherence induced by geometric distortions, thereby highlighting the coherent changes caused by targets of interest.

II. Theory

The estimation of coherence between subsets s_1 and s_2 of two complex SAS images I_1 and I_2 is

$$|\hat{\gamma}| = \frac{\left|\sum_{i=1}^{N} s_1 s_2^*\right|}{\sqrt{\sum |s_1|^2 \sum |s_2|^2}}, \tag{1}$$

where $N = m \times n$ is the number of pixels used for the spatial average. Usually, $|\hat{\gamma}|$ is simply denoted as γ.

Consider the classic interferometer shown in Figure 1, where the point on the seafloor P at height h_1 and displacement d_1 from the reference seafloor is seen from two positions (denoted by blue and red dots) at an altitude A off the seafloor and at ranges R_1 and R_2 respectively, and θ_1 is the elevation angle as seen from P. The baseline B at tilt angle from vertical α is shown, as well as the *perpendicular* baseline $B_\perp$, which is the effective distance between the two looks measured

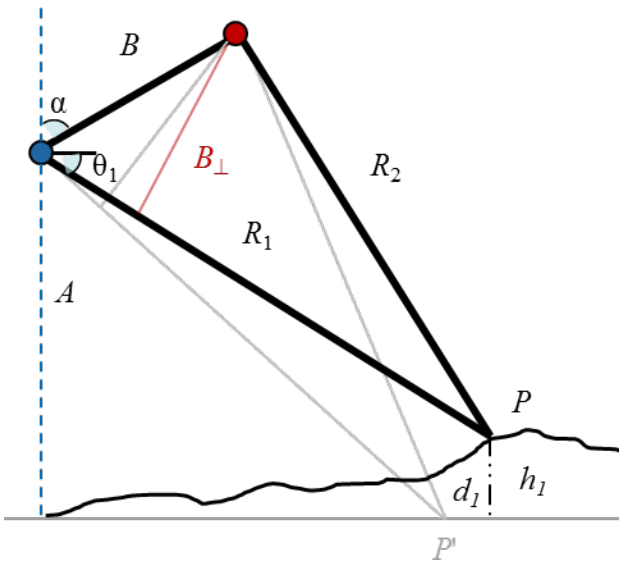

Fig. 1. Typical geometry of an interferometer. The lines R_1 and R_2 indicate the range from an arbitrary point P on the seabed to the position of the sonar on subsequent passes 1 (blue dot) and 2 (red dot). The baseline is denoted by the line B with perpendicular component $B_\perp$.

perpendicular to the look direction [4]. The height of point h_1 is

$$h_1 \approx \frac{R_1\,\phi}{4\pi}\frac{\lambda}{B}\cos\alpha, \tag{2}$$

where $\phi = \frac{4\pi}{\lambda}\Delta R$ is the interferometric phase between R_1 and R_2. By applying (2) for all ranges, one can create a bathymetric map of the seafloor. The influence of d_1 and h_1 on the interferometric phase is such that

$$\phi = \frac{4\pi}{\lambda}\left(B\sin(-\theta_0-\alpha) - d_1 - \frac{B_{\perp,0}}{R_1\cos\theta_1}h_1\right), \tag{3}$$

where θ_0 and $B_{\perp,0}$ are analogous to θ_1 and $B_\perp$, but seen from the reference point P'. One can see from (3) that for fixed h_1, an increase in the baseline B increases the interferometric phase ϕ. In [5], it was shown that the standard deviation on the phase is

$$\sigma_\phi = \frac{1}{2\pi}\frac{\lambda}{2}\frac{1}{\sqrt{n_s}}\sqrt{\frac{1}{\rho}+\frac{1}{\rho^2}}, \tag{4}$$

where n_s is the number of samples used in the averaging to determine the phase and ρ is the signal-to-noise ratio that is related to the measured coherence by $\rho = \frac{1}{1-\gamma}$.

Consider the values for the AquaPix on the Arctic Explorer AUV with $\lambda = 5$ mm and $B = 0.13$ m, at a range $R_1 = 150$ m and an altitude $A = 25$ m. The interferometric phase (2) for a height h_1 of 5 cm is $\phi = 5.7°$. Using (3) with a desired bathymetric resolution of 10×10 cm, one obtains $\sigma_\phi = 5.6°$. If the value of B is increased to one meter, one obtains $\phi = 43.7°$ which is easily measurable. Some well-known results are confirmed here: (i) increases in B result in greater accuracy in vertical measurements (3); and (ii) there is a trade-off between horizontal and vertical accuracy (4). Also, higher coherence results in better estimation of the interferometric phase. Sources for loss of coherence include: temporal coherence due to the highly dynamic underwater environment (*e.g.* turbulence, changes in sound speed, and biological activity); baseline decorrelation caused by differences in the incidence angles of the two images; drops in coherence due to noise and reverberation, such as multipath; and misregistration errors. Of these factors, temporal decorrelation is likely be the most difficult to overcome, since the environment decays faster at the higher frequencies used for high resolution seabed imaging [6].

When two looks are acquired simultaneously on a single platform, the creation of the bathymetric map is relatively straightforward [7] and most sources of decorrelation mentioned above, except possibly multipath, are negligible, and much of the effort is associated with the phase unwrapping problem. In practical systems, the value of B will be determined by the amount of space available on the platform. For most AUVs, this will be on the order of several decimeters. An altnerative approach is to use repeat-pass processing on two images that are acquired from two different sonar passes. This way, arbitrary values of B may be achieved.

In order to process two SAS images interferometrically they must be co-registered to within 1/10 of the theoretical resolution in both horizontal directions. Across track resolution is typically achieved by transmitting a broadband signal, such as a linear frequency modulated chirp, and applying a matched filter to the received echoes, resulting in an across track resolution δ_y of [10]

$$\delta_y = \frac{c}{2\beta}, \tag{5}$$

where $c \approx 1500$ m s^{-1} is the speed of sound in water and β is the bandwidth of the transmitted pulse. Thus, a bandwidth of 50 kHz, which is easily achievable using commercial off-the-shelf (COTS) transducer and electronics technology, results in 1.5 cm across track resolution. The along track resolution δ_x of a SAS is

$$\delta_x = \frac{L_t}{2}, \tag{6}$$

where L_t is the equivalent along track length of the transmitter. Equation (6) demonstrates the desirable property that SAS resolution is independent of both range and frequency. Thus, a transmitter length of 5 cm results in 2.5 cm along track SAS resolution. The necessary accuracy for repeat-pass coregistration is therefore on the order of millimeters for both along and across track directions.

The method used in this paper originates from [8], which is based on classic SAR methods [9] where an iterative method is used to progressively refine the precision of the co-registration. First, a *global* co-registration is done, based on vehicle navigation and detecting the peak cross-correlation between the two images. A simple translation is then applied. The next step involves dividing both images into resolution cells and estimating the *local* along track displacement using wideband cross-correlation. An 11-point truncated sinc interpolation filter is used to correct the along track misregistration. Next, the local across track displacement is estimated and corrected using truncated sinc interpolation. The sequential operations of along track and across track coregistration can be iterated as many times as desired. Finally, (1) is used to estimate the coherence between the two locally coregistered images.

Fig. 2. Deployment of the Arctic Explorer AUV in Bedford Basin, Nova Scotia. The AquaPix transducer array is installed in the payload section aft of the nose cone.

III. Experimental Results

A. Sea trial

AquaPix is a wideband 300 kHz interferometric SAS featuring a unique dual row design for multipath suppression [11]. The sonar was integrated into an Arctic Explorer AUV manufactured by International Submarine Engineering [12]. As shown in Figure 2, the vehicle was deployed from a jetty at the Bedford Institute of Oceanography to collect survey data in Bedford Basin, Nova Scotia, for a joint research project on repeat-pass interferometry with DRDC.

One of the objectives was to determine the maximum allowable separation between passes by measuring the coherence as a function of altitude. A series of rectangular circuits were flown at altitudes of 12.7, 12.9, 13.6, 14.5, and 17.2 m, resulting in 10 repeat-pass image pairs with 9 distinct baseline lengths (the altitude difference of 0.9 m occurs twice). Figure 3 shows a SAS seabed image from the 12.9 m pass generated by Kraken's GPU-accelerated imaging software, which is part of the company's INSIGHT software suite. The mean seabed slope, as measured by InSAS bathymetry, was 1.4°. It can be seen that the selected region is generally flat and featureless, except for a truncated cone target at (25, 30) m across/along track and a scour mark running diagonally across the image.

B. Coherence estimation

The repeat-pass coherence after global coregistration is shown in Figure 4. The vehicle remained submerged during the 19 minute interval between passes. Thus, the translational error between passes is solely due to the drfit of the DVL-aided inertial navigation system and the accuracy with which the vehicle control system follows the desired trajectory. The repeat-pass heading difference measured by the navigation system was 0.05°. The along track and across track displacements estimated by global coregistration were 0.27 and 0.26 m, respectively.

The along track displacement from local coregistration is shown in Figure 5. The globally coregistered complex SAS images from each pass were divided into 0.5 m resolution cells. The along track displacement for each cell was estimated by cross-correlating complex data from corresponding cells using the peak correlation amplitude to measure displacement.

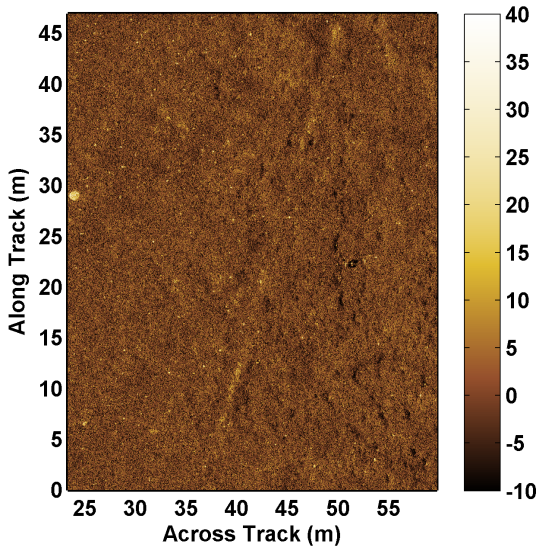

Fig. 3. AquaPix SAS seabed image of the region selected for repeat-pass analysis. The image is from the survey at 12.9 m altitude. The colour scale indicates backscatter intensity in dB normalized by the median value.

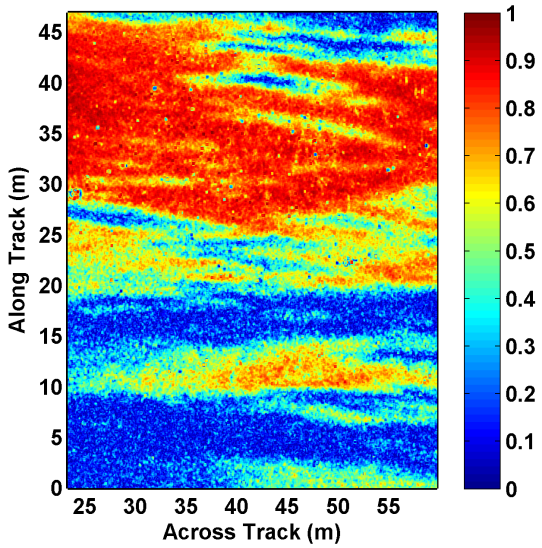

Fig. 4. Repeat-pass coherence after global coregistration. The coherence between SAS images was computed at 25×25 cm resolution.

The along track misregistration was corrected by interpolating one of the repeat-pass images using an 11-point truncated sinc filter and the displacement map shown in Figure 5. The local coregistration procedure was then repeated in the across track direction using the same 0.5 m resolution cells. The residual across track displacement from local coregistration is shown in Figure 6.

As before, the across track misregistration was corrected using truncated sinc interpolation and the displacement map shown in Figure 6. At this stage, the repeat-pass image pair is globally and locally coregistered with subpixel accuracy. The repeat-pass coherence was computed on a 25×25 cm grid

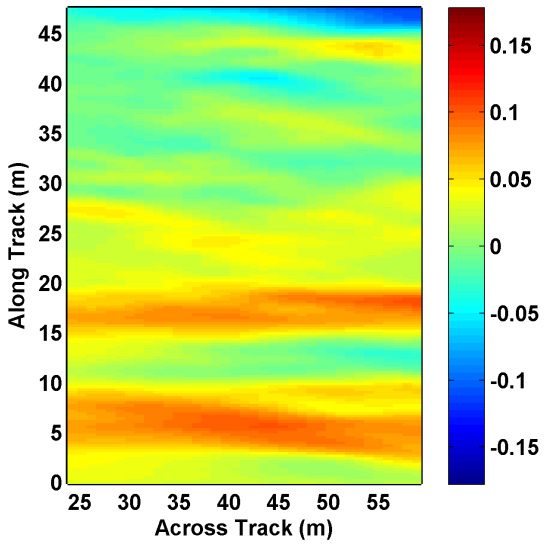

Fig. 5. Along track displacement estimate in meters after local coregistration.

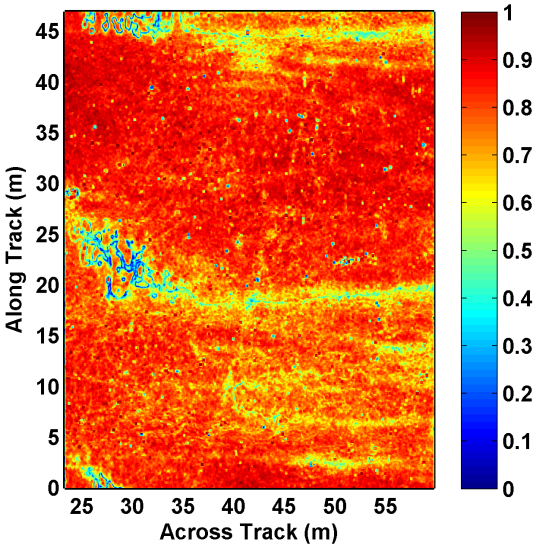

Fig. 7. Repeat-pass coherence after local coregistration. The coherence between SAS images was computed at 25×25 cm resolution.

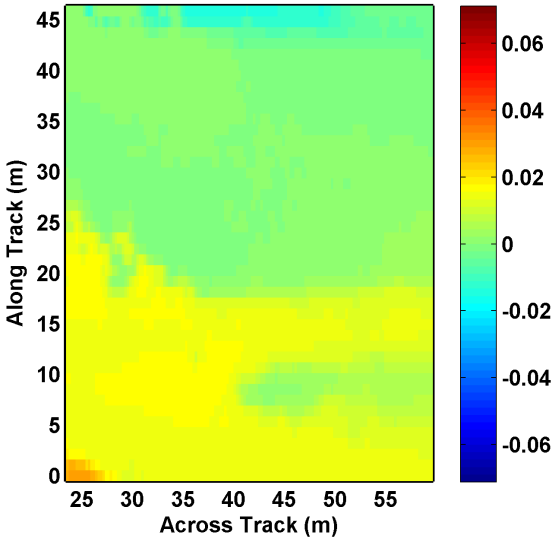

Fig. 6. Across track displacement estimate in meters after local coregistration. The along track displacement from Figure 5 was corrected using truncated sinc interpolation prior to across track local coregistration.

using (1). The coherence after global and local coregistration is shown in Figure 7. It is also possible to select a finer grid for the final coherence computation. For example, equally satisfactory results were obtained on 12×12 cm and 6×6 cm grids, although the interferometric phase becomes noisier on finer grids according to (4).

IV. Conclusion

In this paper, a simple method has been presented for estimating the coherence between repeated passes of a SAS. The method allows estimation at the centimeter-scale without need for deploying reference targets, reprocessing SAS images, or post-processing data from an inertial navigation system. Computational efficiency results from only requiring the coregistration of two complex SAS images and applying an interpolation filter to one of the images. Since SAS images can be focused using relatively low cost angular rate sensors, the method is suitable for vehicles lacking a high grade navigation system, or for the case where raw data is unavailable for post-processing. Also, local coregistration can compensate for a wide class of image distortions including low order geometric effects such as rotation, scaling, and shear.

Results were presented for AquaPix, a wideband 300 kHz interferometric SAS that was integrated into an Arctic Explorer AUV for sea trials in Bedford Basin, Nova Scotia. The repeat-pass imagery were collected for trajectories flown with a vertical separation of 0.7 m and an interval of 19 minutes between passes. Repeat-pass coherence based on global image coregistration showed regions of decoherence that appeared as bands spanning the across track extent of the image. Image warping techniques based on low order polynomials and splines produced similar results. Local image coregistration revealed bands of along track misregistration on the order of ±10 cm, which coincided with rapid variations in AUV altitude. After correcting for along track displacement with a truncated sinc interpolation filter, the residual across track misregistration errors varied between −2 and +3 cm. After a second stage of interpolation to correct across track misregistration, the resulting mean repeat-pass coherence increased to 0.78 compared to 0.51 for global coregistration. The source of the remaining decoherence after local coregistration requires further investigation to determine if it is caused by platform motion or other causes such as interference (acoustic or electrical) or temporal decorrelation (*e.g.* biological activity).

One of the advantages of SAS image processing is that artifacts from platform motion are largely removed from the resulting imagery. However, the coherence results demonstrate that repeat-pass interferometry is sensitive to subtle distortions induced by platform instability that are otherwise

undetectable in the SAS imagery. For example, the vehicle altitude dynamics were not apparent in either Figure 3 or its corresponding repeat-pass image pair. The technique presented here consisted of sequential coregistrations performed in the along track and across track directions. In the case of a more extreme combination of along and across track misregistration, there could be insufficient coherence to reliably estimate the displacement correction required for interpolation. A desirable generalization of the local coregistration technique could involve two-dimensional cross-correlation of resolution cells to simultaneously estimate the along and across track misregistration components.

ACKNOWLEDGMENT

We thank the PISCES2 team from DRDC Atlantic, Fleet Diving Unit Atlantic, the Bedford Institute of Oceanography, and Kraken Sonar Systems for supporting the SAS sea trial.

REFERENCES

[1] V. Myers, D. Sternlicht, A.P. Lyons and R.E. Hansen, "Automated seabed change detection using synthetic aperture sonar: current and future directions," in Proc. 3rd International Conference on SAS and SAR, Lerici, Italy, September 17–19, 2014.

[2] R. De Paulis *et al.,* "SAS multipass interferometry for monitoring seabed deformation using a high-frequency imaging sonar," in Proc. IEEE OCEANS, Santander, Spain, June 6–9, 2011, pp. 1–10.

[3] T. Sæbo, R. Hansen, H. Callow and S. Synnes, "Coregistration of synthetic aperture sonar images from repeated passes," in Proc. Underwater Acoustic Measurements, Kos, Greece, June 20–24, 2011, pp. 1–8.

[4] R.F. Hanssen, *Radar Interferometry,* Kluwer Academic Publishers, 2010.

[5] A. Bellettini and M. Pinto, "Theoretical accuracy of synthetic aperture sonar micronavigation using a displaced phase-center antenna," IEEE Journal of Oceanic Engineering, vol. 27, no. 4, 2002, pp. 780–789.

[6] A.P. Lyons and D.C. Brown, "The impact of the temporal variability of seafloor roughness on synthetic aperture sonar repeat pass interferometry," IEEE Journal of Oceanic Engineering, vol. 38, 2013, pp. 91–97.

[7] T. Sæbo, "Seafloor depth estimation by means of interferometric synthetic aperture sonar," Ph.D. dissertation, University of Tromsø, Norway, 2010.

[8] V. Myers, I. Quidu, T. Sæbo and R. Hansen, "Results and analysis of coherent change detection experiments using repeat-pass synthetic aperture sonar images," in Proc. Underwater Acoustic Measurements, Corfu, Greece, June 23–28, 2013, pp. 613–620.

[9] M. Preiss and N.J.S. Stacey, "Coherent change detection: theoretical description and experimental results", DSTO-TR-1851, 2006.

[10] M.A. Richards, *Fundamentals of Radar Signal Processing,* chap. 8, McGraw-Hill, 2005.

[11] M. Pinto, "Interferometric synthetic aperture sonar design optimized for high area coverage shallow water bathymetric survey," in Proc. Underwater Acoustic Measurements, Kos, Greece, June 20–24, 2011, pp. 1–7.

[12] T. Crees *et al.,* "UNCLOS under ice survey – An historic AUV deployment in the Canadian high arctic," in Proc. OCEANS 2010 Conference, Seattle, WA, September 20–23, 2010, pp. 1–8.